

# Massive Differencing of GNSS Pseudorange Measurements

Helena Calatrava<sup>1</sup>, Daniel Medina<sup>2</sup> and Pau Closas<sup>1</sup>

**Abstract**—Global Navigation Satellite Systems (GNSS) is a popular positioning solution able to provide high accuracy, integrity, reliability and high coverage. GNSS performance may be enhanced through aiding systems such as Differential GNSS (DGNSS), which aims to mitigate disruptive sources of error by using corrections sent from a reference station. In this paper, we investigate a method that provides performance results comparable to those by DGNSS without the need for a reference station. We propose the Massive User-Centric Single Difference (MUCSD) algorithm, which leverages a set of collaborative receivers exchanging observables and, potentially, their noisy estimates of position and clock bias. MUCSD is implemented as an iterative weighted least squares (WLS) estimator and its lower accuracy bound, as given by the Cramér-Rao Bound (CRB), is derived as a performance benchmark for the WLS solution. Simulation results are provided as a function of the number of collaborative users and the exchanged information uncertainty. Results show that, without having to access costly-to-maintain reference stations, MUCSD asymptotically outperforms DGNSS as the number of collaborative receivers grows.

**Index Terms**—Differential GNSS, Collaborative Positioning, Iterative weighted least squares, Cramér-Rao Bound

## I. INTRODUCTION

A wide range of current and future applications demand reliable knowledge of user position [1], such as Intelligent Transportation Systems (ITS) (traffic monitoring, drone tracking, autonomous driving, Vehicle-to-Everything (V2X)), eHealth (patient tracking, emergency equipment location) and Industry 4.0 applications [2]. The integrity, reliability, high coverage and wide deployment provided by Global Navigation Satellite Systems (GNSS) make it a popular solution for positioning [3], [4]. GNSS is able to provide high accuracies under certain conditions, which depend on factors like receiver quality, atmospheric effects, multipath propagation and satellite availability [5]. With the objective of assisting GNSS under the presence of these eventualities, receivers often make use of aiding systems. This is the case of assisted GNSS (A-GNSS), Real-Time Kinematic (RTK) and Differential GNSS (DGNSS). Furthermore, to address the need for high accuracy and continuity of position information required by the aforementioned applications, cooperative positioning and sensor data fusion help stabilizing absolute position and baseline

estimates under challenging conditions (e.g., tunnels and urban canyons) [6], [7].

GNSS-only cooperative and collaborative systems are also explored in the state-of-the-art literature [8]–[10]. Cooperative positioning (CP) exploits location information from additional measurements between users and thus increases localization accuracy. Cooperation between receivers may even help in the task of interference management and classification [11], [12]. One of the main challenges of standard CP solutions is to provide accurate positioning when a subset of receivers is in GNSS-denied conditions, for which multidimensional scaling (MDS) techniques may be employed [13]. Some studies focus on the theoretical limits of CP in the GNSS field. For example, in [14], the Cramér-Rao Bound (CRB) for hybrid CP where GNSS information is combined with terrestrial range measurements is assessed. In [15], IVRs are measured by using raw GNSS observables, which is a similar approach to Differential GNSS (DGNSS), with the difference that both nodes are mobile and there is no presence of a reference or base station, plus only the inter-user range is estimated. Furthermore, it is possible to extract auxiliary inter-vehicular ranges under non-line-of-sight (NLOS) conditions between collaborative receivers by relying only on GNSS observables with Inter-Agent Range (IAR) techniques [10], [16], which use angle measurements from the observation of a common satellite by two collaborative receivers [17]. The study of distributed data-allocation schemes for CP algorithms is also of increasing interest, as it provides flexibility in data processing [18]. Another important aspect of CP is related to the privacy of collaborative agents, which was explored for instance in [19].

The use of both code and carrier-phase measurements for GNSS-only CP is also being investigated [20], [21]. Carrier-phase measurements are more precise but given their high computational cost, they are not always the first option when it comes to GNSS CP algorithms. We focus on the algorithms of the type presented in [8] and [9]. These algorithms suggest that, by using only GPS pseudorange measurements, positioning accuracy can be improved in cooperative vehicular localization systems, which is critical for Cooperative Vehicle Safety (CVS) applications. The standard Double Difference (DD) pseudorange solution is adapted to low-end navigation level GPS receivers for its wide availability in ground vehicles. The carrier-to-noise density ratio (C/N<sub>0</sub>) of raw pseudorange measurements is taken into account for noise mitigation and is used to build the covariance matrix of the proposed weighted least squares (WLS) estimator.

This work has been partially supported by the National Science Foundation under Award ECCS-1845833.

<sup>1</sup>Helena Calatrava and Pau Closas are with Dept. of Electrical and Computer Eng., Northeastern University, Boston, MA (USA). E-mail: {calatrava.h, closas}@northeastern.edu

<sup>2</sup>Daniel Medina is with Institute of Communications and Navigation, German Aerospace Center (DLR), Neustrelitz, Germany. E-mail: daniel.ariasmedina@dlr.de

Tropospheric and ionospheric delays are strong sources of error that affect the performance of GNSS positioning algorithms. Multi-frequency users can cancel the ionospheric delay via the so-called ionosphere-free combination of GNSS measurements, while single-frequency users depend on ionospheric correction models such as Klobuchar in the case of GPS and Nequick in the case of Galileo. Alternatively, single-frequency users can avoid using those model-based ionospheric corrections (which have inherent errors) when GNSS augmentation techniques such as the classical Differential GNSS (DGNS) are used. DGNS uses Single Difference (SD) of pseudorange measurements between the target receiver whose coordinates are unknown and a closeby base station whose coordinates are known with very high accuracy. The main objective of these techniques is to cancel, or at least mitigate, sources of error introduced by the satellite clock and ephemeris prediction, as well as atmospheric delays. The potential error magnitude of such atmospheric sources is on the order of 2 to 10 meters, while it can be reduced to decimeter level after system augmentation is applied under short baseline conditions (i.e., distance between base station and receiver under 10 km) [22]. Although reference stations are the standard solution to provide correction services, reference station networks are extended throughout large areas and consequently they are costly to deploy and maintain. Also, some harmful sources of error cannot be mitigated by DGNS, as they are uncorrelated between receivers, or even between antennae of the same receiver. The latter is the case of errors introduced by multipath propagation. These errors are out of the scope of this research.

In this paper, we propose a collaborative DGNS scheme that does not necessarily require the presence of a well-located reference station. Our objective is to derive and implement a method that provides a performance enhancement comparable to the one provided by DGNS without the need for DGNS corrections, or equivalently, without the need for precise knowledge about the position of a reference station. The hypothesis posed in this research states that it is possible to increase GNSS accuracy with corrections provided by  $N$  collaborative users that have partial knowledge of their positions. We will assume that we are provided with noisy observations of their position and clock bias (through, for instance, a simple undifferenced single point positioning solution) and also with their pseudorange measurements. The proposed Massive User-Centric Single Difference (MUCSD) algorithm [23] aims to estimate the unknown parameter vector of a target receiver, which includes its position and clock bias.

The remainder of this paper is structured as follows. The scheme, observation model and WLS estimator of the proposed MUCSD algorithm for collaborative positioning are described in Section II. The lower accuracy bound of the proposed estimator, as given by the CRB, is derived in Section III. Section IV presents the simulation results, where MUCSD is compared against the lower accuracy bound, the classical DGNS performance and global DGNS performance. Finally, Section V provides a conclusion.

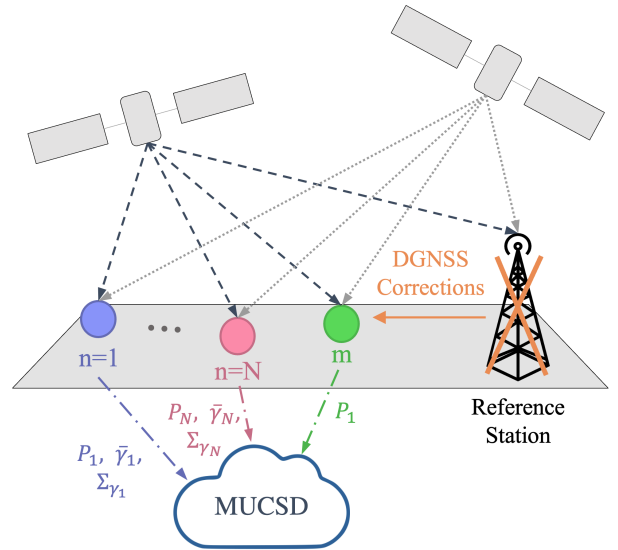


Fig. 1. Proposed scheme for the Massive User-Centric Single Difference (MUCSD) algorithm, where  $N$  collaborative receivers send (1) noisy observations of their position and clock bias  $\bar{\gamma}_n$ , (2) the error covariance matrix of these noisy observations  $\Sigma_{\gamma_n}$  and (3) their pseudorange measurements  $\mathbf{P}_n$  to the cloud. The target user  $m$  also sends its pseudorange measurements  $\mathbf{P}_m$ .

## II. MASSIVE USER-CENTRIC SINGLE DIFFERENCE (MUCSD)

In the proposed scenario,  $N$  collaborative receivers provide (1) noisy observations of their position and clock bias, (2) the error covariance matrix of these noisy observations and (3) their pseudorange measurements to the cloud, where the proposed Massive User-Centric Single Difference (MUCSD) algorithm is running. An illustration of the proposed system can be found in Figure 1. User  $m$  refers to the target user with respect to which the differentiation of pseudorange measurements is calculated. We denote  $\gamma_m = [\mathbf{p}_m^T, c\delta t_m]^T$  as the unknown parameter vector of user  $m$ , where  $\mathbf{p}_m = [x_m, y_m, z_m]^T$  corresponds to the true user position in ECEF coordinates and  $c\delta t_m$  is the receiver clock bias. The aim of the MUCSD algorithm is to estimate the parameter vector  $\gamma_m$  without any prior knowledge and also without the need of DGNS corrections sent by a reference station. It is assumed that users are under short baseline conditions.

### A. Observation Model

MUCSD computes single differentiation between the pseudorange measurements of the target user  $m$  and the  $N$  collaborative receivers. The pseudorange measurements between reference user  $m$  and satellite  $k$  can be expressed as

$$P_m^k = \rho_m^k + c(\delta t_m - \delta t^k) + \eta_m^k, \quad (1)$$

where  $\rho_m^k = \|\mathbf{p}_m - \mathbf{p}^k\|$  is the true range between user  $m$  and satellite  $k$ ,  $\delta t_m$  and  $\delta t^k$  are the receiver and satellite clock biases and  $\eta_m^k = c\Delta T_m^k + c\Delta I_m^k + \epsilon_m^k$ , being  $\Delta T_m^k$  and  $\Delta I_m^k$  the non-dispersive tropospheric delay and the frequency-dependent ionospheric delay terms, respectively. The term

$\epsilon_m^k \sim \mathcal{N}(0, \sigma_\rho^2)$  takes into account errors from various sources such as multipath, ephemeris and relativistic effects. It is considered that for a same receiver the realizations of this error are independent and identically distributed (*i.i.d.*) for different satellites. For simplicity, it is assumed that the pseudorange error standard deviation  $\sigma_\rho$  is the same for the target and collaborative receivers.

Given the non-linearity in  $\rho_m^k$  and if  $h_m^k(\gamma_m) = \rho_m^k + c(\delta t_m - \delta t^k)$ , the expression in (1) can be linearized with respect to  $\gamma = \gamma_0$  by a first-order Taylor approximation and extended to the number of satellites in view  $K$  as

$$\mathbf{P}_m \approx \mathbf{h}(\gamma_{0,m}) + \mathbf{H}(\gamma_m - \gamma_{0,m}) + \boldsymbol{\eta}_m, \quad (2)$$

where  $\mathbf{H}$  is the measurements model matrix from the conventional GNSS positioning algorithms.

In the proposed scheme, the position and clock bias of the collaborative users are known with an error modeled as  $\boldsymbol{\eta}_{\gamma_n} \sim \mathcal{N}(0, \boldsymbol{\Sigma}_{\gamma_n})$ , which we refer to as *collaborative noise* and whose covariance matrix is assumed to be diagonal and common between collaborative receivers, i.e.,  $\boldsymbol{\Sigma}_{\gamma_n} = \sigma_\gamma^2 \mathbf{I}_4 \forall n = \{1, \dots, N\}$ . The collaborative noise standard deviation  $\sigma_\gamma$  may vary depending on the positioning solution used by the collaborative users. It would be potentially interesting to address the benefit of using a fully-populated covariance matrix instead of a diagonal one, exploring whether the tradeoff between communication requirements and positioning performance gain could be showcased. The noisy observations of a collaborative user  $n$  can be expressed as  $\bar{\gamma}_n = [\bar{\mathbf{p}}_n^T, c\delta\bar{t}_n]^T = \gamma_n + \boldsymbol{\eta}_\gamma \sim \mathcal{N}(\gamma_n, \sigma_\gamma^2 \mathbf{I}_4)$ , where  $\gamma_n$  contains the user true position and clock bias. The pseudorange measurements of user  $n$  can also be approximated by a first-order Taylor expansion as

$$\begin{aligned} \mathbf{P}_n &\approx \mathbf{h}(\bar{\gamma}_n) + \mathbf{H}(\gamma_n - \bar{\gamma}_n) + \boldsymbol{\eta}_n \\ &= \mathbf{h}(\bar{\gamma}_n) + \mathbf{H}\boldsymbol{\eta}_\gamma + \boldsymbol{\eta}_n, \end{aligned} \quad (3)$$

where  $\mathbf{P}_n$  has been linearized with respect to  $\bar{\gamma}_n$  so that the error term  $\boldsymbol{\eta}_\gamma$  shows in the expression and its contribution to the covariance matrix can be calculated in a straightforward manner. Given the geometry of the problem, it can be assumed that the line-of-sight (LOS) vectors of matrix  $\mathbf{H}$  are approximately the same between receivers (i.e.,  $\mathbf{H}$  from (2) and (3) is approximately the same). Combining (2) and (3), the single differentiation of pseudorange measurements between the target receiver  $m$  and a collaborative receiver  $n$  is calculated as  $\Delta\mathbf{P}_{m,n} = \mathbf{P}_m - \mathbf{P}_n$ , which results in

$$\Delta\mathbf{P}_{m,n} \approx \mathbf{h}(\gamma_{0,m}) + \mathbf{H}(\gamma_m - \gamma_{0,m}) - \mathbf{h}(\bar{\gamma}_n) + \boldsymbol{\epsilon}_{m,n}, \quad (4)$$

where the tropospheric and ionospheric delays have been canceled due to the differentiation between two users in a short baseline scenario (distances under 10 km). The error vector  $\boldsymbol{\epsilon}_{m,n} = \boldsymbol{\epsilon}_m - \boldsymbol{\epsilon}_n - \boldsymbol{\epsilon}_\gamma$  includes the difference between the pseudorange error of the two users,  $\boldsymbol{\epsilon}_m \sim \mathcal{N}(0, \sigma_\rho^2 \mathbf{I}_K)$  and  $\boldsymbol{\epsilon}_n \sim \mathcal{N}(0, \sigma_\rho^2 \mathbf{I}_K)$ , and also the resulting error from the

collaborative noise,  $\boldsymbol{\epsilon}_\gamma = \mathbf{H}\boldsymbol{\eta}_\gamma \sim \mathcal{N}(0, \sigma_\gamma^2 \mathbf{H}\mathbf{H}^T)$ . A linear observation model can be built from (4) as follows

$$\begin{aligned} \mathbf{y}_{m,n} &= \Delta\mathbf{P}_{m,n} - \mathbf{h}(\gamma_{0,m}) + \mathbf{h}(\bar{\gamma}_n) \\ &= \mathbf{H}(\gamma_m - \gamma_{0,m}) + \boldsymbol{\epsilon}_{m,n}. \end{aligned} \quad (5)$$

Considering that  $\bar{\boldsymbol{\Gamma}}_{1:N} = [\bar{\gamma}_1 \ \bar{\gamma}_2 \ \dots \ \bar{\gamma}_N]^T$ , the model in (5) can be expanded to the case of  $N$  user pairs as

$$\begin{aligned} \mathbf{y} &= \Delta\mathbf{P} - \mathbf{1}_{N \times 1} \otimes \mathbf{h}(\gamma_{0,m}) + \mathbf{h}(\bar{\boldsymbol{\Gamma}}_{1:N}) \\ &= \mathbf{A}(\gamma_m - \gamma_{0,m}) + \boldsymbol{\epsilon}. \end{aligned} \quad (6)$$

where  $\mathbf{A} = \mathbf{1}_{N \times 1} \otimes \mathbf{H}$ . These observations can be modeled as  $\mathbf{y} \sim \mathcal{N}(\boldsymbol{\mu}, \boldsymbol{\Sigma})$ , where  $\boldsymbol{\mu} = \mathbf{A}\gamma_m$  if the term  $\mathbf{A}\gamma_{0,m}$  is moved to the left side of the expression in (6).

### B. Error Covariance Matrix

The error vector  $\boldsymbol{\epsilon}_{m,n}$  can be expanded to  $N$  instances of single differentiation as

$$\boldsymbol{\epsilon} = \mathbf{1}_{N \times 1} \otimes \boldsymbol{\epsilon}_m - \boldsymbol{\epsilon}_{1:N} - (\mathbf{I}_N \otimes \mathbf{H})\boldsymbol{\eta}_{\gamma_{1:N}}. \quad (7)$$

Therefore, the error covariance matrix has dimension  $NK \times NK$  and can be calculated as

$$\begin{aligned} \boldsymbol{\Sigma} &= \mathbb{E}[\boldsymbol{\epsilon}\boldsymbol{\epsilon}^T] = \mathbb{E}[(\mathbf{1}_{N \times 1} \otimes \boldsymbol{\epsilon}_m)(\mathbf{1}_{N \times 1} \otimes \boldsymbol{\epsilon}_m)^T]^{(a)} \\ &\quad + \mathbb{E}[\boldsymbol{\epsilon}_{1:N}\boldsymbol{\epsilon}_{1:N}^T]^{(b)} \\ &\quad + \mathbb{E}[(\mathbf{I}_N \otimes \mathbf{H})\boldsymbol{\eta}_{\gamma_{1:N}}((\mathbf{I}_N \otimes \mathbf{H})\boldsymbol{\eta}_{\gamma_{1:N}})^T]^{(c)}. \end{aligned} \quad (8)$$

The first term (8) (a) corresponds to

$$\begin{aligned} &\mathbb{E}[(\mathbf{1}_{N \times 1} \otimes \boldsymbol{\epsilon}_m)(\mathbf{1}_{N \times 1} \otimes \boldsymbol{\epsilon}_m)^T] \\ &= \mathbf{J}_{N \times N} \otimes \sigma_\rho^2 \mathbf{I}_K, \end{aligned} \quad (9)$$

where  $\mathbf{J}_{N \times N}$  is the all-ones matrix with dimension  $N \times N$ . Regarding the second term (8) (b) and considering the aforementioned assumptions, we obtain  $\mathbb{E}[\boldsymbol{\epsilon}_{1:N}\boldsymbol{\epsilon}_{1:N}^T] = \sigma_\rho^2 \mathbf{I}_{NK}$ . Finally, regarding the third term (8) (c) is derived as

$$\begin{aligned} &\mathbb{E}[(\mathbf{I}_N \otimes \mathbf{H})\boldsymbol{\eta}_{\gamma_{1:N}}((\mathbf{I}_N \otimes \mathbf{H})\boldsymbol{\eta}_{\gamma_{1:N}})^T] \\ &= (\mathbf{I}_N \otimes \mathbf{H})\mathbb{E}[\boldsymbol{\eta}_{\gamma_{1:N}}\boldsymbol{\eta}_{\gamma_{1:N}}^T](\mathbf{I}_N^T \otimes \mathbf{H}^T) \\ &= \sigma_\gamma^2 \mathbf{I}_N \otimes \mathbf{H}\mathbf{H}^T. \end{aligned} \quad (10)$$

Consequently, the error covariance matrix of the MUCSD observation model can be expressed as

$$\boldsymbol{\Sigma} = \sigma^2(\mathbf{J}_{N \times N} \otimes \mathbf{I}_K + \mathbf{I}_{NK}) + \sigma_\gamma^2 \mathbf{I}_N \otimes \mathbf{H}\mathbf{H}^T. \quad (11)$$

### C. Iterative WLS Solution

As observations are non-*i.i.d.*, a weighting matrix  $\mathbf{W} = \boldsymbol{\Sigma}^{-1}$  is required for the WLS estimator as

$$\hat{\gamma}_m = (\mathbf{A}^T \mathbf{W} \mathbf{A})^{-1} \mathbf{A}^T \mathbf{W} \mathbf{y}. \quad (12)$$

Due to the non-linearity in the pseudorange measurement expression, this is a non-linear Least Squares problem. Consequently, it is necessary to solve the estimator iteratively by

linearizing the function at some initial guess  $\gamma_{0,m}$ . A new estimate at time  $j$  can be computed as

$$\begin{aligned}\hat{\gamma}_m^{j+1} &= \begin{bmatrix} \mathbf{P}_m^{j+1} \\ c\delta t_m^{j+1} \end{bmatrix} \\ &= \begin{bmatrix} \mathbf{P}_m^j \\ 0 \end{bmatrix} + (\mathbf{A}^{j\top} \mathbf{W}^j \mathbf{A}^j)^{-1} \mathbf{A}^{j\top} \mathbf{W}^j \mathbf{y}^j,\end{aligned}\quad (13)$$

where the superscript  $j$  in  $\mathbf{W}^j$  and  $\mathbf{A}^j$  indicates that these matrices change at each iteration, as they are dependent on matrix  $\mathbf{H}$ . The LOS vectors in matrix  $\mathbf{H}$  draw an imaginary line between the receiver and the satellite and consequently change for different values of  $\mathbf{p}_m^j$ . For this stochastic model, the WLS estimator is equivalent to the Maximum Likelihood Estimator (MLE) because the observations belong to a Gaussian distribution.

### III. PERFORMANCE BOUND

The lower accuracy bound of the estimator in (12) as given by the CRB is derived as a performance benchmark for the proposed WLS solution. The Fisher Information Matrix (FIM) is calculated as

$$\mathcal{I}(\gamma_m) = -\mathbb{E} \left[ \frac{\partial^2 \ln f(\mathbf{y}|\gamma_m)}{\partial \gamma_m \partial \gamma_m^\top} \right] = \mathbf{A}^\top \Sigma^{-1} \mathbf{A}, \quad (14)$$

and therefore the CRB for element  $[\hat{\gamma}_m]_i$  can be obtained as

$$\begin{aligned}\text{var}([\hat{\gamma}_m]_i) &\geq \text{CRB}([\hat{\gamma}_m]_i) \\ &= [(\mathbf{A}^\top \Sigma^{-1} \mathbf{A})^{-1}]_{ii}.\end{aligned}\quad (15)$$

MUCSD performance is also compared to DGNSS (i.e., when a base station of known coordinates and clock bias is available) and to what we refer to as Global DGNSS, which assumes that there is available knowledge on the coordinates of  $N$  base stations.

We also define a performance *global bound (GB)*, which is an ideal bound equivalent to the bound provided by DGNSS under the assumption that the pseudorange error of the base station is negligible. This equates to the MUCSD algorithm for  $N = 1$  (i.e., one collaborative user, which would correspond to the reference station), with  $\sigma_\gamma = 0$  and  $\sigma_\rho = 0$  for the collaborative receiver, which provides the following lower accuracy bound

$$\begin{aligned}\text{var}([\hat{\gamma}_m^{\text{GB}}]_i) &\geq \text{CRB}_{\text{GB}}([\hat{\gamma}_m^{\text{GB}}]_i) \\ &= [(\mathbf{H}^\top \Sigma_{\text{GB}}^{-1} \mathbf{H})^{-1}]_{ii} \text{ s.t. } \Sigma_{\text{GB}} = \text{diag}(\sigma_\rho^2).\end{aligned}\quad (16)$$

This bound differs from the DGNSS CRB, as with DGNSS the pseudorange error variances are added up, and consequently  $\Sigma_{\text{DGNSS}} = \text{diag}(2\sigma_\rho^2)$ .

## IV. RESULTS

### A. Experimental Setup

Experimental results are provided in this section. A scenario is simulated with  $K = 7$  satellites in view and in common between the target user and the  $N$  collaborative users. A total of  $N + 1$  users are uniformly distributed with a maximum inter-user distance of 200 meters for each ECEF coordinate.

In Section IV-B, the performance of the MUCSD estimator provided in (12) is compared to (a) the estimator lower bound in (15), (b) the DGNSS CRB and (c) the ideal global bound described in (16) as a function of a pseudorange error standard deviation  $\sigma_\rho$  between 1 and 20 meters.

To demonstrate the effectiveness of the proposed algorithm, results are shown for an increasing number of collaborative users  $N$  in Section IV-C. The estimator in (12) is compared to (a), (b), (c) and also to the performance provided by (d) Global DGNSS. We discuss results obtained for  $N = 2, 10, 50$  and 100 under varying  $\sigma_\rho$  and also for an increasing number of collaborative users up to 2000. MUCSD performance is studied under different values of  $\sigma_\gamma$ , namely 0 (low), 10 and 20 (moderate), and 100 (high) meters.

### B. Influence of the pseudorange noise

Figure 2 shows the performance of the MUCSD algorithm as a function of the pseudorange error standard deviation  $\sigma_\rho$ . In the scenario proposed by the left subfigure, we are assuming that the position and clock bias of the collaborative receivers are known with a noise of standard deviation  $\sigma_\gamma = 10$  meters. Under these conditions and with only one collaborative user, the MUCSD algorithm is not able to achieve the DGNSS bound. However, for  $N = 2$  and 10 the DGNSS bound is achieved at approximately  $\sigma_\rho = 7.5$  and 3 meters, respectively. The right figure scenario, with  $\sigma_\gamma = 100$  meters, is a very pessimistic case. However, the MUCSD algorithm is able to outperform DGNSS for  $N = 50$  and 100 users at  $\sigma_\rho = 11.5$  and 8.5 meters, approximately. This leads to the conclusion that the algorithm introduced in this paper is able to reach DGNSS performance regardless of the collaborative noise value, for an increasing value of  $N$  collaborative receivers. Consequently, MUCSD is further assessed as a function of  $N$  in the following section for the two values of  $\sigma_\rho$  indicated in Figure 2 (left), being (a)  $\sigma_\rho = 2$  meters and (b)  $\sigma_\rho = 15$ .

The MUCSD bound gets closer to the GB defined in (16) for high values of  $N$  and  $\sigma_\rho$ . For example, for  $\sigma_\gamma = 10$  meters, the variance difference between MUCSD and GB is around 3 meters and remains constant for  $N = 10$  and  $\sigma_\rho > 4$  meters. Moreover, it can be seen how MUCSD approaches GB for high values of  $N$  and  $\sigma_\rho$  even under very pessimistic conditions, when  $\sigma_\gamma = 100$  meters, for  $N = 50$  and 100 collaborative users.

### C. Influence of the number of collaborative users

In Figure 3, the MUCSD algorithm performance under a varying number of collaborative users  $N$  is shown for  $\sigma_\rho = 2$  (left subfigure) and  $\sigma_\rho = 15$  (right subfigure) meters. Results provided by the global DGNSS model (i.e., assuming that there is available knowledge on the coordinates of  $N$  base stations) are the ones in green ( $\sigma_\gamma = 0$  meters). The gap between MUCSD and DGNSS is higher for low values of  $\sigma_\rho$  and mostly for low values of  $N$ . For instance, for  $\sigma_\rho = 2$  meters, and  $N = 5$ , DGNSS outperforms MUCSD when  $\sigma_\gamma = 10$  meters by approximately 3 meters. However, for  $\sigma_\rho = 15$  meters and  $N = 5$ , MUCSD when  $\sigma_\gamma = 10$

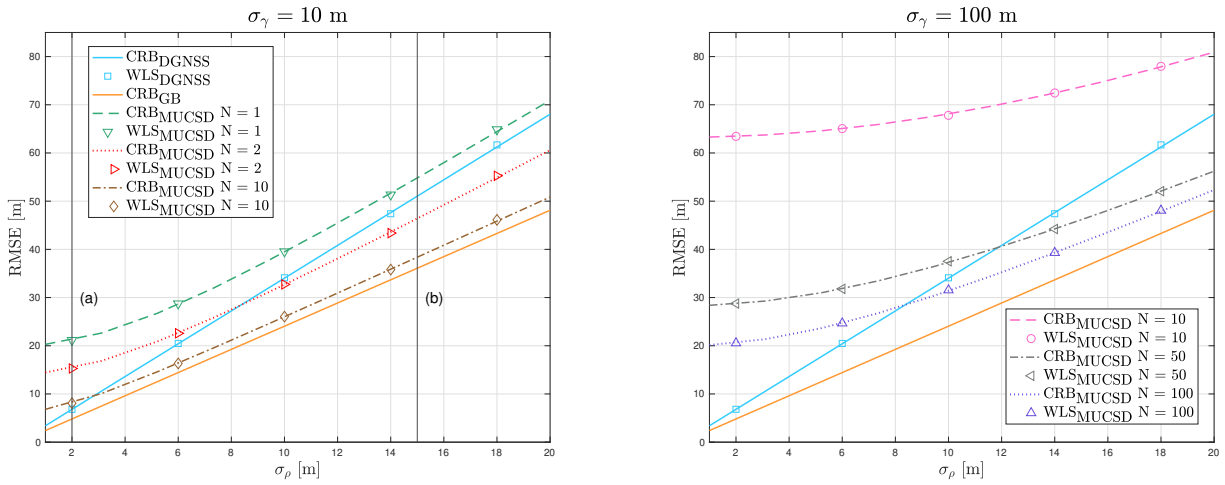


Fig. 2. MUCSD performance under varying pseudorange error standard deviation  $\sigma_\rho$  (between 1 and 20 meters) and for two values of collaborative noise standard deviation  $\sigma_\gamma$ , namely 10 m (left) and 100 m (right). In the left figure, (a) and (b) indicate the two values of  $\sigma_\rho$  under study in Figure 3.

meters outperforms DGNSS by approximately 15 meters. Also when  $\sigma_\rho = 15$ , even for moderate values of  $\sigma_\gamma$  such as 20 meters the MUCSD algorithm asymptotically reaches DGNSS performance for a low number of collaborative users (less than 5). Nevertheless, achieving GB is more challenging, as both Global DGNSS and MUCSD need  $N > 40$  for that purpose.

When  $\sigma_\rho = 2$  and for a moderate value of  $\sigma_\gamma = 10$  meters, MUCSD reaches DGNSS for  $N = 20$ , but for  $\sigma_\gamma = 20$  meters, we are not able to see when DGNSS performance is achieved. In order to answer the question of whether the MUCSD algorithm can reach DGNSS performance for low values of  $\sigma_\rho$  and high values of  $\sigma_\gamma$ , we can inspect Figure 4.

Figure 4 shows the performance of the MUCSD algorithm under a varying number of collaborative users, but this time for very high values of  $N$  (between 200 and 2000). Tested values of collaborative noise standard deviation are also very high (and pessimistic). For  $\sigma_\gamma = 75$  meters, the MUCSD bound reaches DGNSS for  $N = 1000$  users, meaning that even with a noise in collaborative observations of 75 meters, our algorithm is able to properly estimate the position and clock bias of the target receiver when  $N = 1000$  collaborative receivers. The same happens for  $\sigma_\gamma = 100$  meters, which although being a very high value of collaborative noise allows the MUCSD algorithm to outperform DGNSS when  $N = 1800$ . Consequently, we can state that the algorithm introduced in this paper is able to asymptotically outperform DGNSS regardless of the magnitude of collaborative noise, for an increasing value of  $N$ .

## V. CONCLUSION

This paper presented a novel algorithm for massive single differentiation of observables that achieves DGNSS performance without the need for a reference or base station. Instead, we showed that it is possible to work with noisy observations of  $N$  collaborative receivers whose positions are not necessarily accurately known. The higher the value of  $N$  the better the

performance is, as shown (both theoretically and experimentally). The algorithm, named as Massive User-Centric Single Difference (MUCSD), is implemented as an iterative weighted least squares (WLS) estimator which is known to be optimal under Gaussian models. The results of MUCSD are compared against the lower accuracy bound, provided by the Cramér-Rao Bound (CRB), the classical DGNSS performance (that is, single differences of a user with observables of a well-located base station), the global DGNSS performance (as a benchmark, this is the case of having  $N$  collaborative users with accurate knowledge of their positions, as in the case of having  $N$  base stations) and an ideal global performance bound defined by the authors. Results show that the proposed scheme asymptotically achieves DGNSS performance for an increasing value of  $N$  and that it can even outperform it depending on the values of  $N$  and the uncertainty in the location of the collaborative users, asymptotically reaching an ideal global performance.

## REFERENCES

- [1] D. Dardari, P. Closas, and P. M. Djurić, "Indoor tracking: Theory, methods, and technologies," *IEEE Transactions on Vehicular Technology*, vol. 64, no. 4, pp. 1263–1278, 2015.
- [2] N. Chukhno, S. Trilles, J. Torres-Sospedra, A. Iera, and G. Araniti, "D2D-Based Cooperative Positioning Paradigm for Future Wireless Systems: A Survey," *IEEE Sensors Journal*, vol. 22, no. 6, pp. 5101–5112, 2022.
- [3] P. Groves, *Principles of GNSS, Inertial, and Multisensor Integrated Navigation Systems, Second Edition*, ser. GNSS/GPS. Artech House, 2013. [Online]. Available: <https://books.google.com/books?id=t94fAgAAQBAJ>
- [4] Y. J. Morton, F. van Diggelen, J. J. Spilker Jr, B. W. Parkinson, S. Lo, and G. Gao, *Position, Navigation, and Timing Technologies in the 21st Century: Integrated Satellite Navigation, Sensor Systems, and Civil Applications*. John Wiley & Sons, 2021.
- [5] N. Williams, P. Borhani Darian, G. Wu, P. Closas, and M. Barth, "Impact of positioning uncertainty on connected and automated vehicle applications," *SAE International Journal of Connected and Automated Vehicles*, vol. 6, 08 2022.

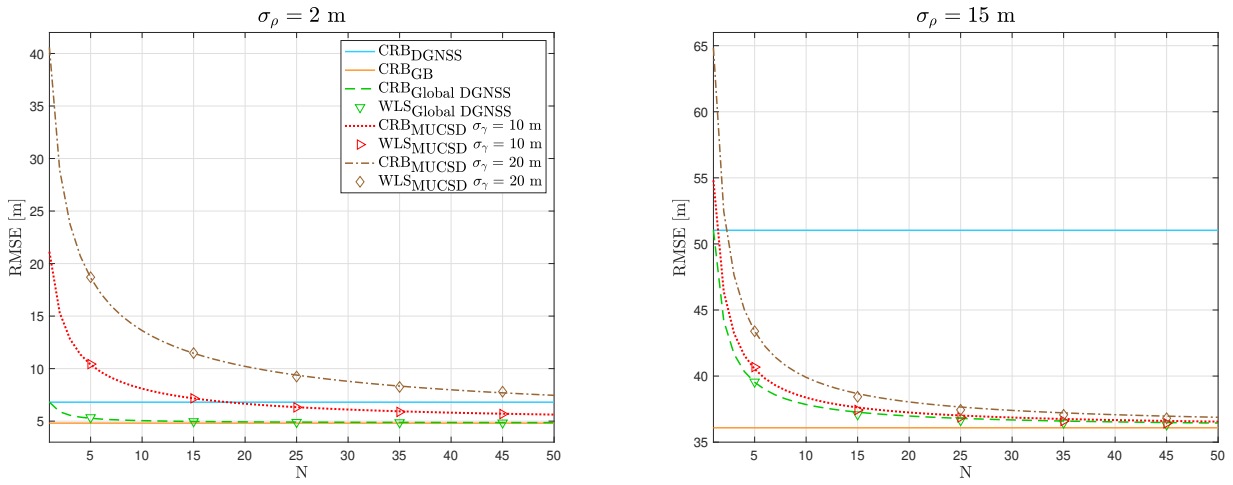


Fig. 3. MUCSD performance under a varying number of collaborative users  $N$  in the scenario (between 1 and 50 users) for two values of  $\sigma_\rho$ , namely 2 m (left) and 15 m (right).

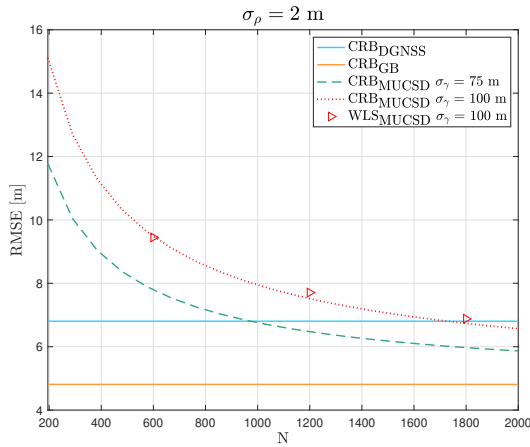


Fig. 4. MUCSD performance under varying number of collaborative users  $N$  (between 200 and 2000 users).

[6] D. Grejner-Brzezinska, C. Toth, T. Moore, J. Raquet, M. Miller, and A. Kealy, "Multisensor Navigation Systems: A Remedy for GNSS Vulnerabilities," *Proceedings of the IEEE*, vol. 104, pp. 1–15, 03 2016.

[7] F. de Ponte Müller, E. Diaz, B. Kloiber, and T. Strang, "Bayesian cooperative relative vehicle positioning using pseudorange differences," 05 2014.

[8] D. Yang, F. Zhao, K. Liu, H. B. Lim, E. Frazzoli, and D. Rus, "A GPS Pseudorange Based Cooperative Vehicular Distance Measurement Technique," in *2012 IEEE 75th Vehicular Technology Conference (VTC Spring)*, 2012, pp. 1–5.

[9] K. Liu, H. B. Lim, E. Frazzoli, H. Ji, and V. C. S. Lee, "Improving Positioning Accuracy Using GPS Pseudorange Measurements for Cooperative Vehicular Localization," *IEEE Transactions on Vehicular Technology*, vol. 63, no. 6, pp. 2544–2556, 2014.

[10] A. Minetto, A. Nardin, and F. Dovis, "Gnss-only collaborative positioning among connected vehicles," 07 2019.

[11] M. Nicola, G. Falco, R. Ferre, E. S. Lohan, A. Fuente, and E. Falletti,

"Collaborative Solutions for Interference Management in GNSS-Based Aircraft Navigation," *Sensors*, vol. 20, p. 4085, 07 2020.

[12] A. Nardin, T. Imbiriba, and P. Closas, "Crowdsourced localization of jammers with an augmented path loss model," in *2023 IEEE/ION Position, Location and Navigation Symposium (PLANS)*. IEEE, 2023.

[13] A. Naouri, L. Ortega, J. Vilà-Valls, and E. Chaumette, "A Multidimensional Scaling Approach for Cooperative GNSS Navigation," in *2021 International Conference on Localization and GNSS (ICL-GNSS)*, 2021, pp. 1–6.

[14] F. Penna, M. A. Caceres, and H. Wymeersch, "Cramér-Rao Bound for Hybrid GNSS-Terrestrial Cooperative Positioning," *IEEE Communications Letters*, vol. 14, no. 11, pp. 1005–1007, 2010.

[15] K. Mazher, M. Tahir, and K. Ali, "GNSS pseudorange smoothing: Linear vs non-linear filtering paradigm," in *2016 IEEE Aerospace Conference*, 2016, pp. 1–10.

[16] A. Minetto, A. Nardin, and F. Dovis, "Tight Integration of GNSS Measurements and GNSS-based Collaborative Virtual Ranging," 10 2018.

[17] A. Minetto and F. Dovis, "A theoretical framework for collaborative estimation of distances among GNSS users," in *2018 IEEE/ION Position, Location and Navigation Symposium (PLANS)*, 2018, pp. 1492–1501.

[18] E. D. Nerurkar, S. I. Roumeliotis, and A. Martinelli, "Distributed maximum a posteriori estimation for multi-robot cooperative localization," in *2009 IEEE International Conference on Robotics and Automation*, 2009, pp. 1402–1409.

[19] G. Hernandez, G. LaMountain, and P. Closas, "Privacy-preserving cooperative positioning," in *Proceedings of the 33rd International Technical Meeting of the Satellite Division of The Institute of Navigation (ION GNSS+ 2020)*, 2020, pp. 2667–2675.

[20] E. Richter, M. Obst, R. Schubert, and G. Wanielik, "Cooperative relative localization using Vehicle-To-Vehicle communications," in *2009 12th International Conference on Information Fusion*, 2009, pp. 126–131.

[21] F. de Ponte Müller, A. Steingass, and T. Strang, "Zero-Baseline Measurements for Relative Positioning in Vehicular Environments," 12 2013.

[22] P. Misra and P. Enge, *Global Positioning System: Signals, Measurements, and Performance*. Ganga-Jamuna Press, 2011. [Online]. Available: <https://books.google.es/books?id=5WJ0yWAACAAJ>

[23] H. N. Calatrava Rodríguez, "Cooperative Positioning using Massive Differentiation of GNSS Pseudorange Measurements," Master's thesis, UPC, Escola Tècnica Superior d'Enginyeria de Comunicacions, Sep 2022. [Online]. Available: <http://hdl.handle.net/2117/373227>